Journal of Geophysical Research: Atmospheres

Supporting Information for

Cascading Delays in the Monsoon Rice Growing Season and Post-Monsoon Agricultural Fires Likely Exacerbate Air Pollution in North India

T. Liu[1], L. J. Mickley[2], P. N. Patel[3,4], R. Gautam[5], M. Jain[6], S. Singh[6], Balwinder-Singh[7], R. S. DeFries[8], and M. E. Marlier[9]

[1]Department of Earth and Planetary Sciences, Harvard University, Cambridge, MA, USA
[2]John A. Paulson School of Engineering and Applied Sciences, Harvard University, Cambridge, MA, USA
[3]Jet Propulsion Laboratory, California Institute of Technology, Pasadena, CA, USA
[4]Oak Ridge Associated Universities, Oak Ridge, TN, USA
[5]Environmental Defense Fund, Washington DC, USA
[6]School for Environment and Sustainability, University of Michigan, Ann Arbor, MI, USA
[7]International Maize and Wheat Improvement Center (CIMMYT)-India Office, New Delhi, India
[8]Department of Ecology, Evolution, and Environmental Biology, Columbia University, New York, NY, USA
[9]Department of Environmental Health Sciences, University of California, Los Angeles, Los Angeles, CA, USA

Contents of this file

S1 Satellite-observed temporal shifts in crop phenology and fire activity

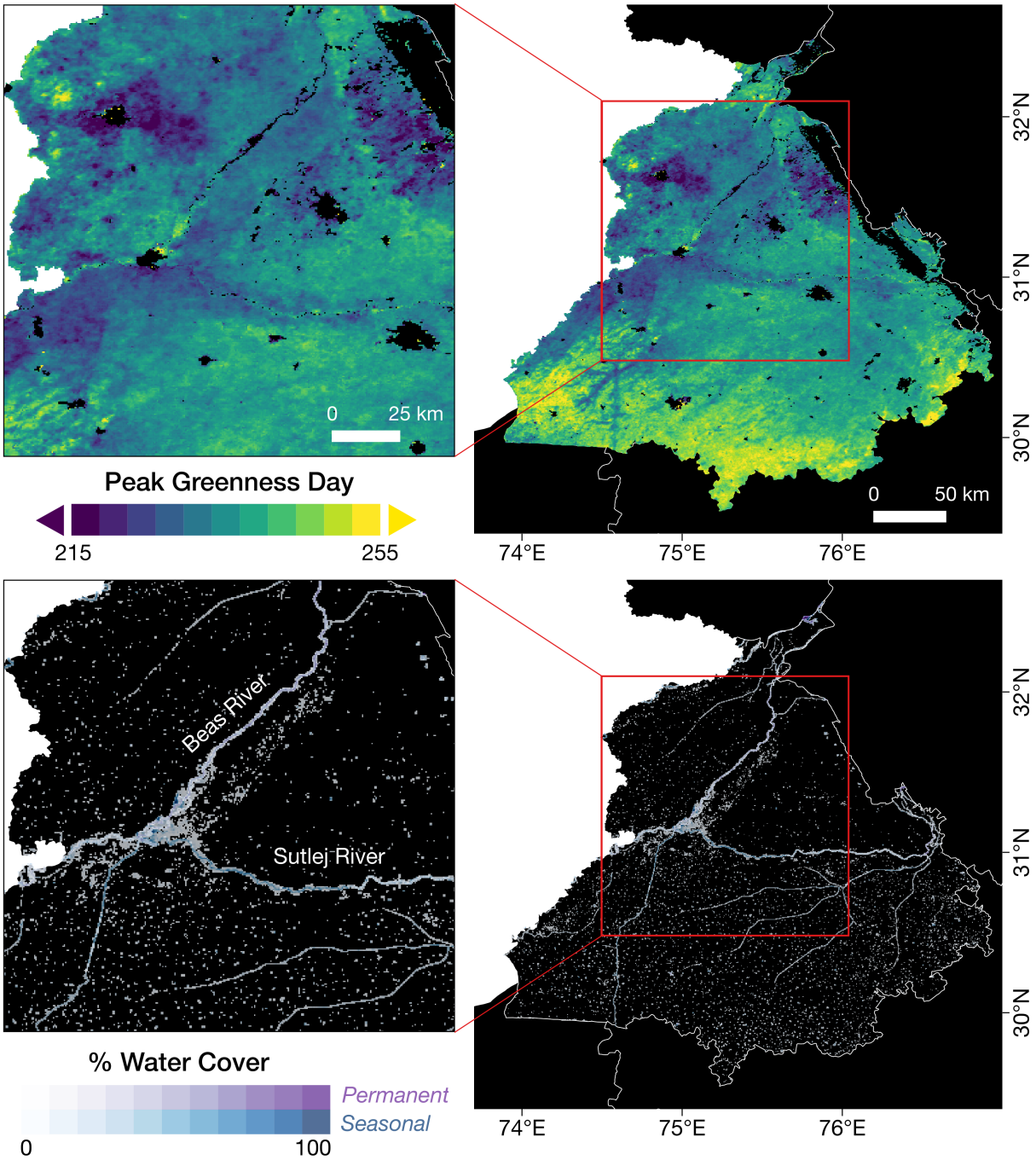

Figure S1. Spatial variability in monsoon crop phenology in Punjab during the 2003-2007 period: (*Top panel*) Day of the year of peak monsoon greenness derived from MODIS MCD12Q2, averaged across 2003-2007. (*Bottom panel*) Location of seasonal (blue shades) and permanent (purple shades) water cover derived from the Copernicus Dynamic Global Land Cover (CGLS-LC100) from 2015-2019. Areas with greatest water coverage (i.e., darkest shades) are located near the intersection of the Beas and Sutlej Rivers. Most of the water cover pixels are classified as seasonal. The CGLS land cover is upsampled to 500 m for visibility.

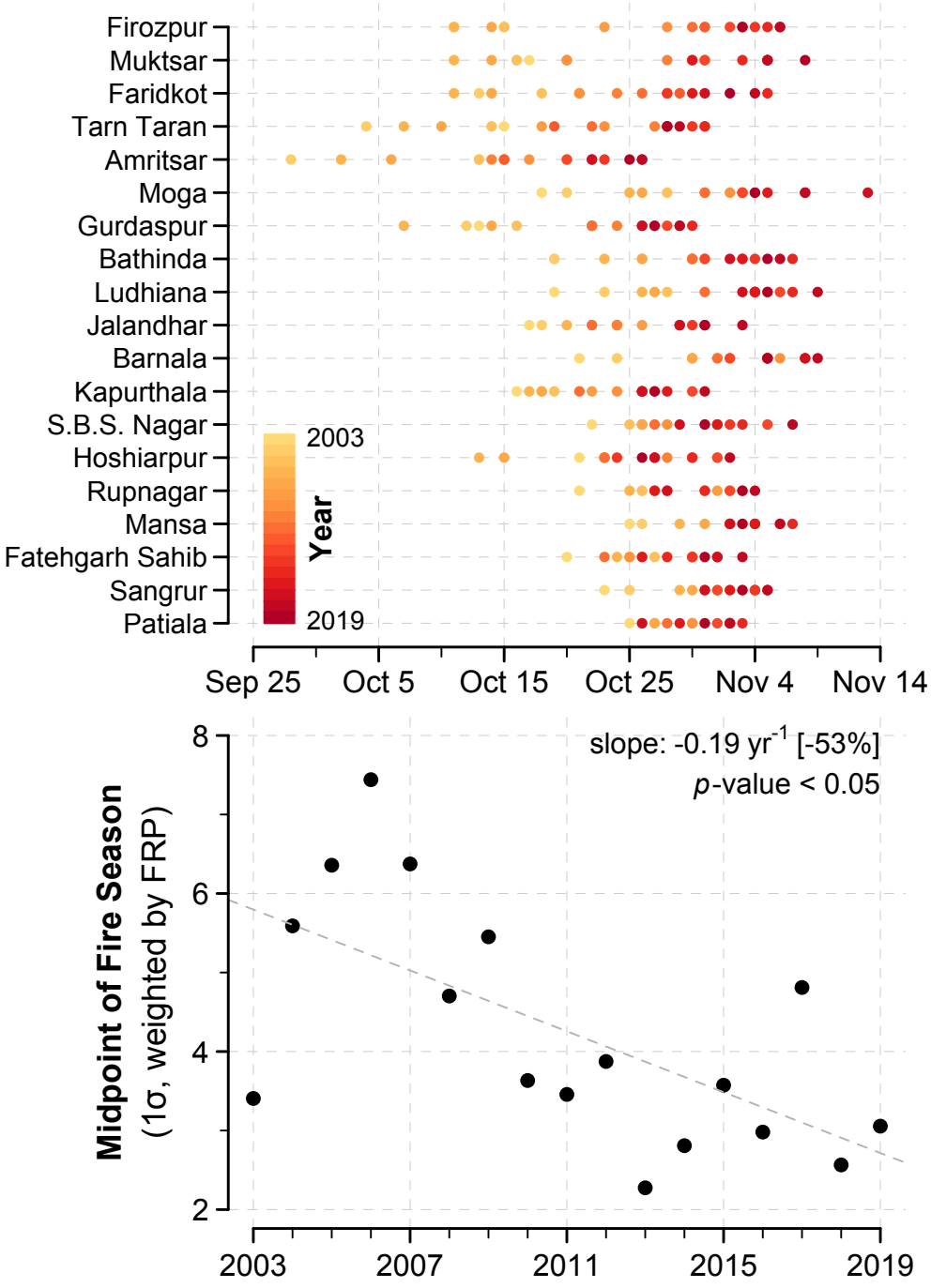

Figure S2. Spatial variability in the midpoint of the post-monsoon fire season among Punjab districts from 2003-2019: (*Top panel*) The midpoint of post-monsoon fire seasons in 19 districts (same as in Figure 1) in Punjab from 2003-2019, colored by year. The districts shown are ordered by the magnitude of the temporal shift, from highest to lowest. (*Bottom panel*) The standard deviation of the spatial distribution of district-level post-monsoon fire season midpoint dates, weighted by the overall FRP of each district, from 2003-2019. The slope and *p*-value of the linear trend are shown inset. The percentage inset indicates the total change in the standard deviation of the midpoint of the fire season from 2003-2019 as derived from the linear trend.

Groundwater levels. In addition to groundwater data from India-WRIS and Dacnet, we use household survey data from the 2017-18 crop season to estimate the usage of canal irrigation in three regions in Punjab: Amritsar (north), Sangrur (southeast), and Bathinda/Muktsar (southwest) districts. 573 households in Punjab are represented in the subset of the household survey we used in this study. Methodology for the household survey is described in Liu et al. (2020).

S1.1 *Spatial heterogeneity in groundwater usage and trends in context of temporal shifts in the monsoon growing season and post-monsoon fires*

Visual inspection of the spatial heterogeneity in peak monsoon greenness at the native MODIS spatial resolution (500 m) reveals that regions with initially early monsoon crop cycles (i.e., in northern and western Punjab), as well as the greatest cascading delays, are near major rivers integral to canal irrigation (Figure S1). Remote sensing and ground measurements suggest that these districts are less affected by groundwater depletion (Asoka et al., 2017). Annual maps of the pre-monsoon depth to water level by India's Central Groundwater Board, based on interpolated well data, show shallower depths in western Punjab (< 20 m) than eastern Punjab (20-40 m) (https://indiawris.gov.in/wris/#/gwyearbook), suggesting more abundant water resources in the west.

Household survey data of irrigation practices collected in 2018 in three Punjab regions (Amritsar, Bathinda/Muktsar, and Sangrur districts) show similar spatial variation (Figure S3). While access to tubewells is nearly universal, canal irrigation is high in southwestern Punjab (Bathinda/Muktsar: 88%) but low in southeastern and northern Punjab (Sangrur: 34%, Amritsar: 11%) (Table S1). Recent structural collapses in the canal networks in districts such as Amritsar may increase groundwater dependence further (The Tribune India, 2019). Although paddy growing depends on groundwater rather than canal irrigation, the latter's availability may have alleviated the water table decline. Aside from differences in irrigation, crop varieties may also contribute to spatial variation in peak monsoon greenness, which is tied to the duration of the growing season (Figure S4). Compared to eastern and central Punjab, farmers in western Punjab tend to plant crops earlier in the season (Figure S1) and favor varieties with shorter growing periods (Figure S4). While western Punjab experienced the greatest delays, farmers there use shorter duration crop varieties, which produce less residue and require less irrigation and may help to reduce fire emissions and offset groundwater use (Dhillon & Kumar, 2021; Mahajan et al., 2009).

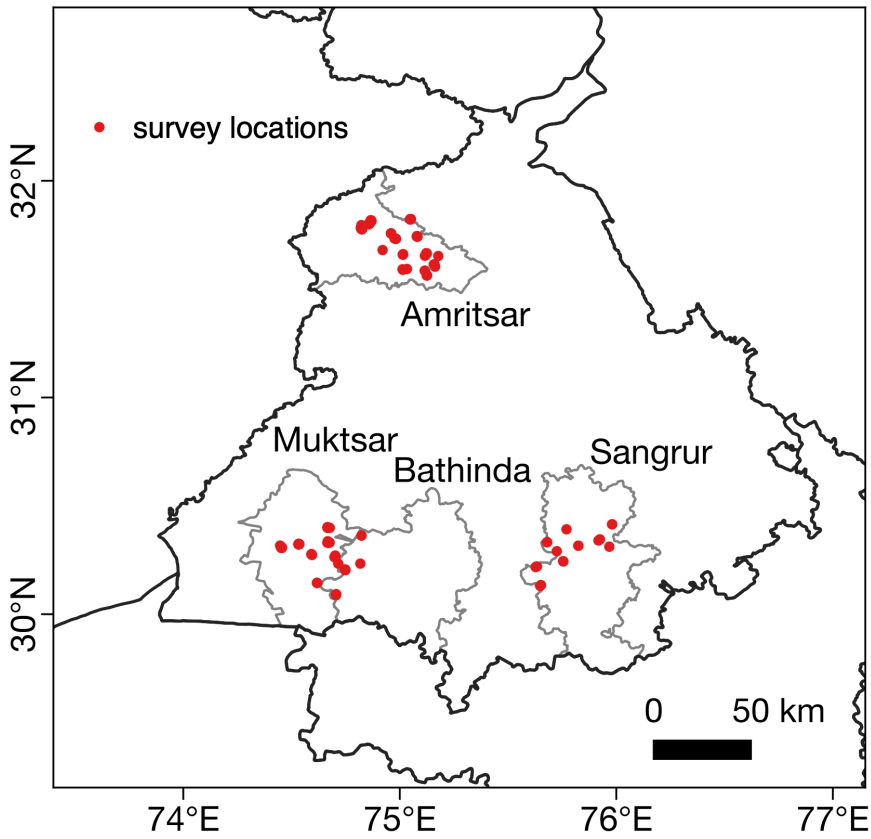

Figure S3. Household survey locations in Punjab: Red dots correspond to household survey locations in Punjab, mainly within the Amritsar, Muktsar, Bathinda, and Sangrur districts.

Table S1. Irrigation practices in Punjab, India by district from household survey data

	Irrigation	**Amritsar**	**Muktsar/ Bathinda**	**Sangrur**
Household survey, 2018	Canal	11%	88%	34%
	Groundwater			
	tubewell, owned	78%	85%	82%
	tubewell, shared	19%	7%	18%
	tubewell, rented	6%	9%	2%

Amritsar (*n*=186), Muktsar/Bathinda (*n*=196), Sangrur (*n*=191)

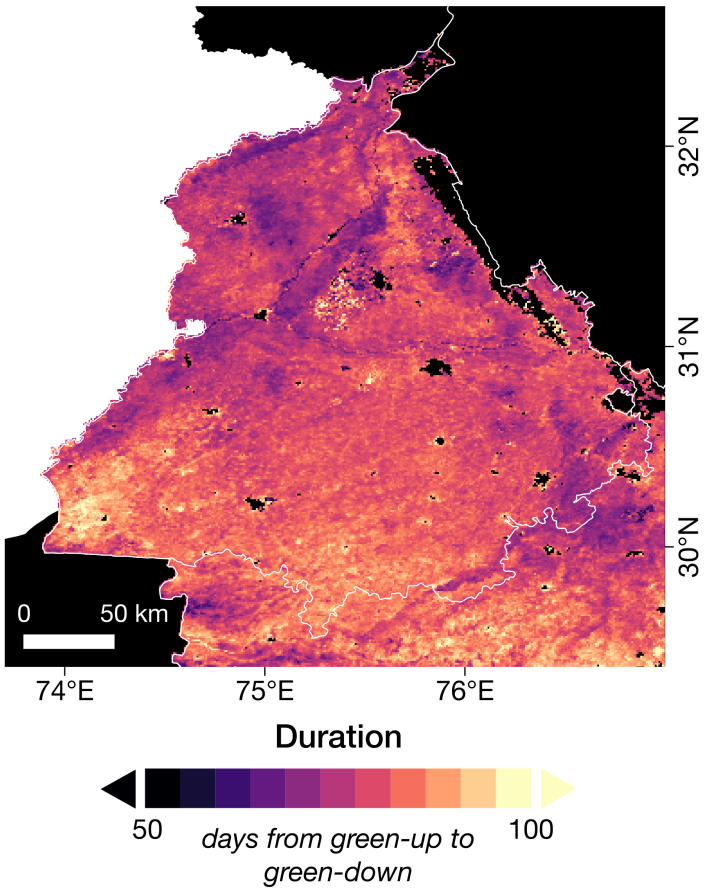

Figure S4. Duration from green-up to green-down during the monsoon growing season in northwest India: average number of days between green-up and green-down from 2003-2019 derived from the MCD12Q2 phenology dataset.

S2 Atmospheric Transport Modeling of Smoke $PM_{2.5}$

S2.1 *STILT Modeling*

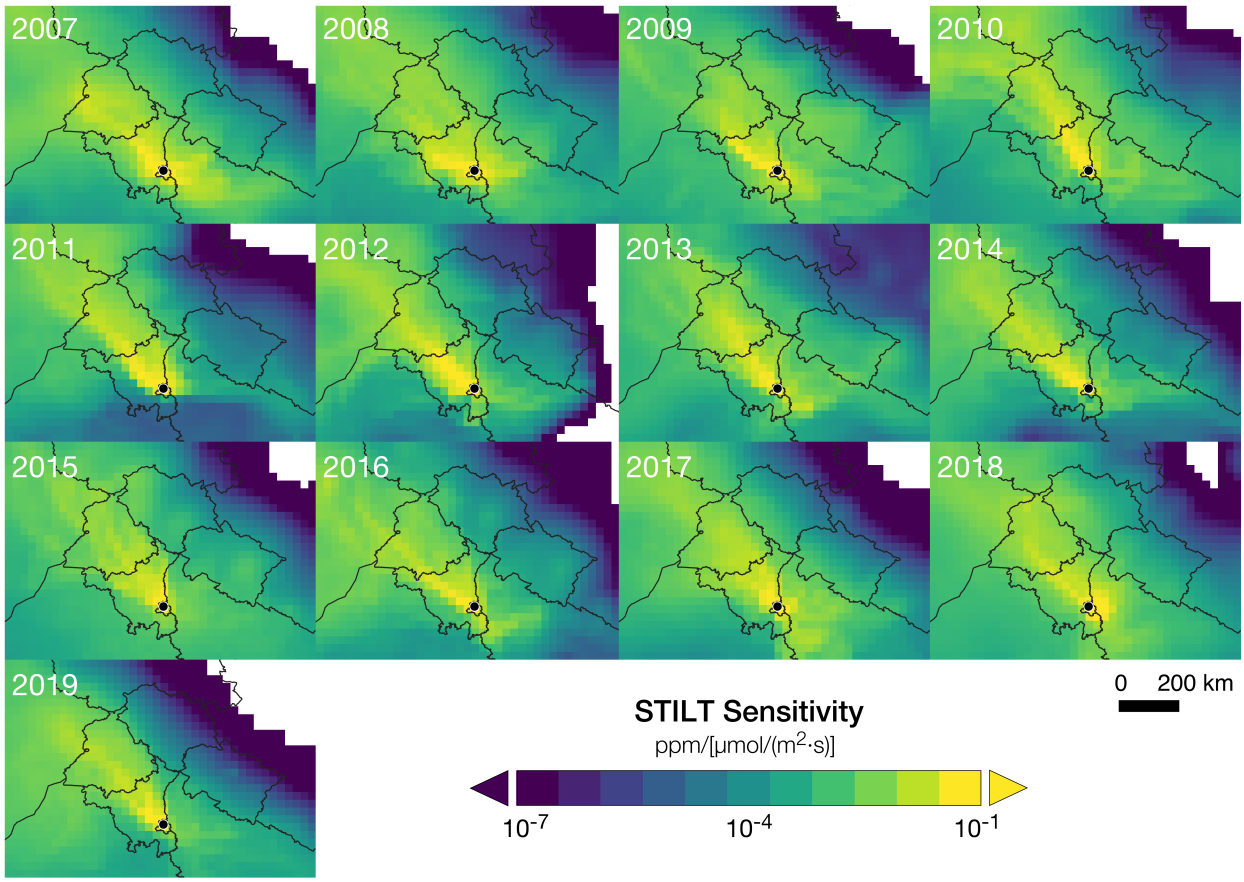

Figure S5. Annual variation in STILT sensitivities from 2007-2019 with New Delhi as the receptor: STILT sensitivity maps are averaged using the daily smoke $PM_{2.5}$ at New Delhi as weights. To calculate the $PM_{2.5}$ weights, STILT sensitivities of a given meteorological year are applied to each year's post-monsoon fire emissions from 2008-2019. The $PM_{2.5}$ is then averaged by day across the fire emissions years to standardize the fire season, account for the delay and increase in fires during this period, and focus the year-to-year comparison of the STILT sensitivities on meteorological patterns.

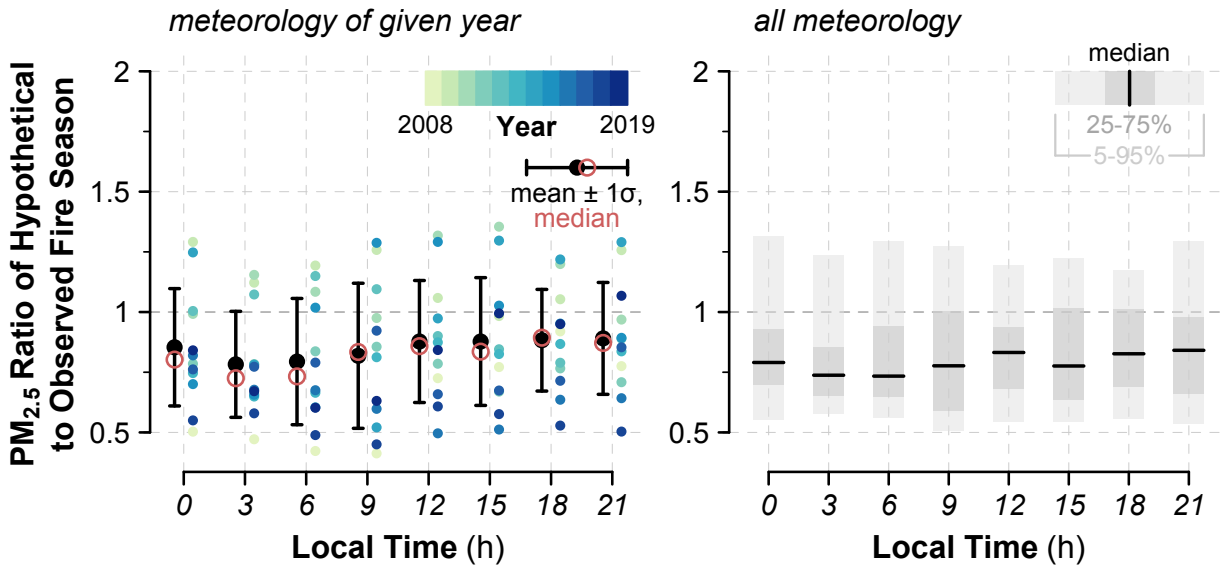

Figure S6. Effect on $PM_{2.5}$ in New Delhi from 2008-2019 if the post-monsoon agricultural fire season had not experienced delays relative to the 2003-2007 period: Fire emissions are shifted earlier by the number of days between the peak burning day of each fire season and that of the 2003-2007 average. Unlike Figure 5, here the STILT-simulated $PM_{2.5}$ ratio is shown for eight different local hours of the day: 0, 3, 6, 9, 12, 15, 18, and 21 h. (*Left panel*) Maximum smoke $PM_{2.5}$ from a 21-day rolling mean from October 1 to November 30 for a hypothetical fire season that is shifted earlier relative to one that was observed. For each hour, the $PM_{2.5}$ ratio is shown as the median (red circles), mean ± 1σ (black dots and bars), and for individual years (colored dots). (*Right panel*) The fire emissions of each year are applied to STILT sensitivities for all years from 2007-2019 to show a range of possible meteorological conditions. The $PM_{2.5}$ ratio is averaged across meteorological years by quantiles. The horizontal bars show the median for each hour; the dark gray envelopes show the 25th-75th percentile range, and the light gray envelopes show the 5th-95th percentile range.

S2.2 *Background $PM_{2.5}$*

We use $PM_{2.5}$ observed at the U.S. Embassy in New Delhi from 2013-2019 to quantify the increase in background $PM_{2.5}$ from October to December. For each year, we use quantile regression to fit a linear trend to the timeseries of daily average $PM_{2.5}$ at the 20th percentile, which results in a fitted line apparently consistent with observations dominated by background $PM_{2.5}$ and not strongly influenced by outliers or by $PM_{2.5}$ spikes associated with crop residue burning. We extend the $PM_{2.5}$ timeseries from October to December to prevent inflation of the estimated trend in background $PM_{2.5}$ due to high $PM_{2.5}$ days during November.

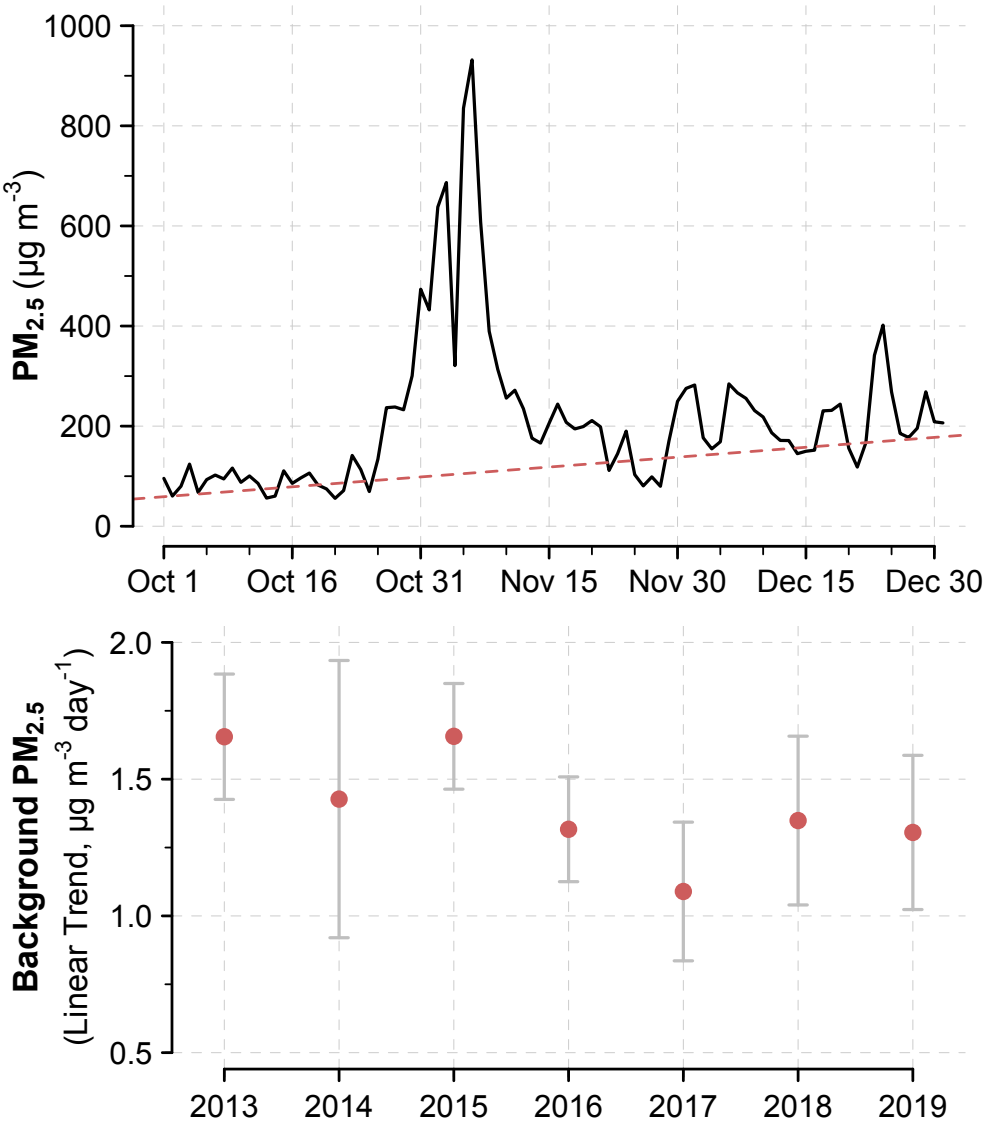

Figure S7. Increase in daily background $PM_{2.5}$ in New Delhi from post-monsoon to winter, 2013-2019: (*Top panel*) Example timeseries of daily average $PM_{2.5}$ (black line) observed at the U.S. Embassy in New Delhi from Oct 1 to Dec 30, 2016. The linear increase in background $PM_{2.5}$ (red dashed line) is estimated using quantile regression at the 20th percentile. (*Bottom panel*) The slope ± 1 standard error of the linear trend in background $PM_{2.5}$ from 2013-2019.

GEOS-Chem chemical transport model (CTM). We use the GEOS-Chem CTM, version 12.8.2 (https://zenodo.org/record/3860693), to simulate daily background $PM_{2.5}$ concentrations for a 3-year period from 2015-2017 (Bey et al., 2001). We use the global 2° x 2.5° full chemistry simulation with a 6-month spin-up to generate boundary conditions for the nested grid simulation (0.5° x 0.625°) of the Asia domain, both driven by MERRA2 reanalysis meteorology (Wang et al., 2004). Anthropogenic emissions are from the MIX inventory for Asia (Li et al., 2017). Fire emissions are from a combined GFEDv4s and SAGE-IGP dataset, with SAGE-IGP replacing GFEDv4s agricultural fire emissions over north India.

We use the GEOS-Chem simulated background $PM_{2.5}$ to calculate how much smoke $PM_{2.5}$ contributes to the total $PM_{2.5}$ at each receptor (Table S2). STILT and GEOS-Chem smoke $PM_{2.5}$ concentrations are consistent for New Delhi, Kanpur, and Bathinda, whereas GEOS-Chem tends to overestimate smoke $PM_{2.5}$ in Lahore, Ludhiana, and Jind relative to STILT. Discrepancies between the models may arise due to differences in spatial resolution and input meteorology. In GEOS-Chem, emissions inventories are first upscaled to the nested grid resolution (0.5° x 0.625°), while in STILT, we generate sensitivity footprints at the native resolution of the SAGE-IGP inventory (0.25° x 0.25°).

In addition, we find that GEOS-Chem is unable to capture the increase in observed background $PM_{2.5}$ as seen by its > 50% underestimate in December compared to October, two months with much less influence from biomass burning than from anthropogenic sources (Figure S8). Such biases in anthropogenic emissions inventories or incomplete chemical mechanisms in the model may in turn lead to underestimates in total $PM_{2.5}$ and highly polluted days in November.

Table S2. Background and smoke $PM_{2.5}$ ($\mu g\ m^{-3}$) in the six receptor cities from 2015-2017. The $PM_{2.5}$ concentrations shown are the maximum of 21-day rolling means from October to November. Ranges within the parentheses refer to the minimum and maximum from 2015-2017. Smoke $PM_{2.5}$ is simulated using STILT and GEOS-Chem, while background $PM_{2.5}$ is simulated only in GEOS-Chem. Here, smoke $PM_{2.5}$ is defined as the sum of primary OC and BC emitted by fires, or 2.1 × OC + BC, to make the STILT and GEOS-Chem estimates consistent. The 2.1 factor converts OC to organic matter, as suggested in Turpin and Lim (2001).

Receptor	**Background $PM_{2.5}$** (GEOS-Chem, no fire simulation)	**STILT**		**GEOS-Chem**	
		Smoke $PM_{2.5}$	%	Smoke $PM_{2.5}$	%
New Delhi	133 (110-173)	32 (27-37)	20 (14-24)	35 (31-40)	21 (18-22)
Kanpur	116 (95-149)	13 (9-20)	10 (6-16)	16 (9-20)	11 (7-15)
Lahore	119 (91-151)	28 (26-30)	20 (15-25)	66 (44-100)	35 (26-47)
Ludhiana	134 (107-166)	39 (18-57)	23 (10-35)	179 (91-235)	55 (35-66)
Bathinda	105 (82-145)	158 (145-179)	61 (51-67)	209 (148-244)	66 (63-73)
Jind	115 (93-152)	64 (50-78)	36 (25-44)	143 (112-176)	56 (42-63)

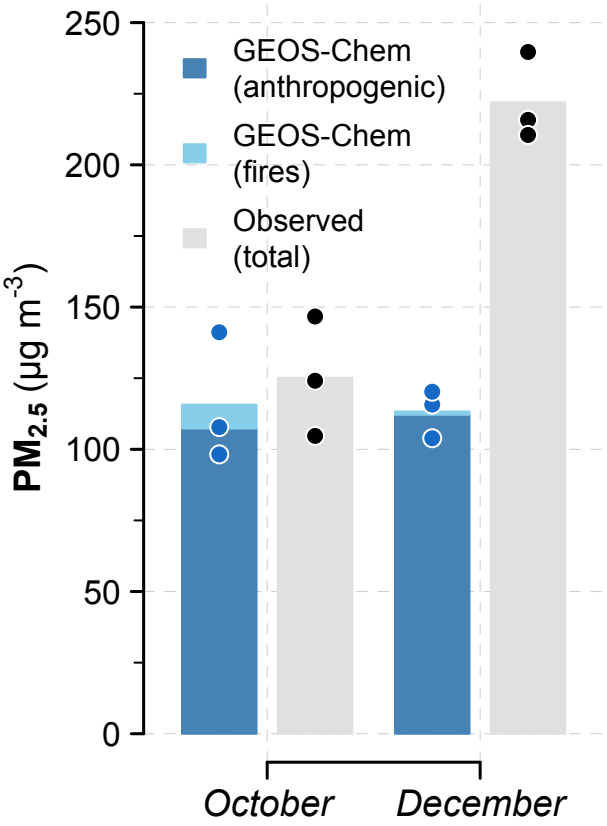

Figure S8. Observed and modeled $PM_{2.5}$ in New Delhi in October and December from 2015-2017: Monthly average $PM_{2.5}$ from observations (gray) and GEOS-Chem nested grid model simulations partitioned into anthropogenic (dark blue) and biomass burning (light blue) sources. Dots represent monthly averages of total $PM_{2.5}$ in individual years.

References

Asoka, A., Gleeson, T., Wada, Y., & Mishra, V. (2017). Relative contribution of monsoon precipitation and pumping to changes in groundwater storage in India. *Nature Geoscience*, *10*(2), 109–117. https://doi.org/10.1038/ngeo2869

Bey, I., Jacob, D. J., Yantosca, R. M., Logan, J. A., Field, B. D., Fiore, A. M., et al. (2001). Global modeling of tropospheric chemistry with assimilated meteorology: Model description and evaluation. *Journal of Geophysical Research Atmospheres*, *106*(D19), 23073–23095. https://doi.org/10.1029/2001JD000807

Dhillon, B. S., & Kumar, R. (2021). Short-duration paddy varieties can turn the tide. *The Tribune India*. Retrieved from https://www.tribuneindia.com/news/punjab/short-duration-paddy-varieties-can-turn-the-tide-264670

Li, M., Zhang, Q., Kurokawa, J. I., Woo, J. H., He, K., Lu, Z., et al. (2017). MIX: A mosaic Asian anthropogenic emission inventory under the international collaboration framework of the MICS-Asia and HTAP. *Atmospheric Chemistry and Physics*, *17*(2), 935–963. https://doi.org/10.5194/acp-17-935-2017

Liu, T., Mickley, L. J., Singh, S., Jain, M., DeFries, R. S., & Marlier, M. E. (2020). Crop residue burning practices across north India inferred from household survey data: bridging gaps in satellite observations. *Atmospheric Environment: X*, *8*, 100091. https://doi.org/10.1016/j.aeaoa.2020.100091

Mahajan, G., Bharaj, T. S., & Timsina, J. (2009). Yield and water productivity of rice as affected by time of transplanting in Punjab, India. *Agricultural Water Management*, *96*(3), 525–532. https://doi.org/10.1016/j.agwat.2008.09.027

The Tribune India. (2019). Crumbling canal system takes toll on groundwater. Retrieved from https://www.tribuneindia.com/news/archive/punjab/crumbling-canal-system-takes-toll-on-groundwater-790245

Turpin, B. J., & Lim, H. J. (2001). Species contributions to PM2.5 mass concentrations: Revisiting common assumptions for estimating organic mass. *Aerosol Science and Technology*, *35*, 602–610. https://doi.org/10.1080/02786820119445

Wang, Y. X., McElroy, M. B., Jacob, D. J., & Yantosca, R. M. (2004). A nested grid formulation for chemical transport over Asia: Applications to CO. *Journal of Geophysical Research: Atmospheres*, *109*(22), D22307. https://doi.org/10.1029/2004JD005237